

DeepMicroClass sorts metagenomes into prokaryotes, eukaryotes and viruses, with marine applications

Shengwei Hou^{1,2\$*}, Tianqi Tang^{3\$}, Siliangyu Cheng^{3\$}, Ting Chen⁴, Jed A. Fuhrman¹, Fengzhu Sun^{3*}

¹ Marine and Environmental Biology, Department of Biological Sciences, University of Southern California, Los Angeles, CA 90089, USA

² Department of Ocean Science and Engineering, Southern University of Science and Technology, Shenzhen 518055, China

³ Quantitative and Computational Biology Department, University of Southern California, Los Angeles, CA 90089, USA

⁴ Department of Computer Science and Technology, Institute of Artificial Intelligence & BNRIst, Tsinghua University, Beijing 100084, China

^{\$} These authors contributed equally to this work.

* Correspondence: housw@sustech.edu.cn (S. Hou) and fsun@usc.edu (F. Sun)

1 Abstract

2 Sequence classification reduces the complexity of metagenomes and facilitates a fundamental understanding of the structure and function of microbial communities. Binary metagenomic classifiers 3 offer an insufficient solution because environmental metagenomes are typically derived from multiple sequence sources, including prokaryotes, eukaryotes and the viruses of both. Here we introduce 4 a deep-learning based (as opposed to alignment-based) sequence classifier, DeepMicroClass, that classifies metagenomic contigs into five sequence classes, i.e., viruses infecting prokaryotic or 5 eukaryotic hosts, eukaryotic or prokaryotic chromosomes, and prokaryotic plasmids. At different 6 sequence lengths, DeepMicroClass achieved area under the receiver operating characteristic curve 7 (AUC) scores >0.98 for most sequence classes, with the exception of distinguishing plasmids from 8 prokaryotic chromosomes (AUC scores ≈ 0.97). By benchmarking on 20 designed datasets with variable 9 sequence class composition, we showed that DeepMicroClass obtained average accuracy scores 10 of ~ 0.99 , ~ 0.97 , and ~ 0.99 for eukaryotic, plasmid and viral contig classification, respectively, which 11 were significantly higher than the other state-of-the-art individual predictors. Using a 1-300 μm 12 daily time-series metagenomic dataset sampled from coastal Southern California as a case study, 13 we showed that metagenomic read proportions recruited by eukaryotic contigs could be doubled 14 with DeepMicroClass's classification compared to the counterparts of other alignment-based classifiers. 15 With its inclusive modeling and unprecedented performance, we expect DeepMicroClass will 16 be a useful addition to the toolbox of microbial ecologists, and will promote metagenomic studies of 17 under-appreciated sequence types.

18 **keywords:** metagenomic contig classification, microbial eukaryotes, eukaryotic viruses, phages, 19 plasmids

20 Introduction

21 Microbes are major players of global biogeochemical cycles owing to their high abundance, immense 22 diversity, versatile metabolism, and survivability in any conceivable ecosystem on the planet (Falkowski 23 et al., 2008; Azam & Worden, 2004). Microbial communities are a collection of diverse biological 24 entities, including ribosome-encoding cellular organisms (REOs), capsid-encoding organisms (CEOs, i.e., 25 viruses) that can only reproduce within cells of REOs, and orphan replicons (plasmids, transposons, etc) 26 that parasitize REOs or CEOs for propagation (Raoult & Forterre, 2008). Viruses and plasmids are 27 extrachromosomal genetic elements that have important implications for the diversity and function of 28 29 30

31 microbial communities owing to their roles in transferring genetic materials between or within microbes.
32 Thus, together with transposable elements, they are collectively referred to as mobile genetic elements
33 (MGEs). Depending on where, when and how metagenomic samples were collected, the microbial di-
34 versity within a sample can range from a consortium of several dominant strains to a conglomerate of
35 thousands of species. Soon after the discovery of the small subunit rRNA gene (SSU) as a universally
36 conserved phylogenetic marker (Woese & Fox, 1977), the biodiversity and structure of environmental
37 microbial communities can be easily assessed using the SSU-based amplicon surveys (Pace et al., 1986;
38 Olsen et al., 1986). Microbial coding potentials can be further probed using cloning libraries of natural
39 microbial assemblages (e.g., cosmid and fosmid libraries) (Olsen et al., 1986; Schmidt et al., 1991; Stein
40 et al., 1996; Vergin et al., 1998; Rondon et al., 2000; Béjà et al., 2000; Legault et al., 2006), which
41 have been revolutionized by shotgun metagenomes to infer functional capabilities and ecological roles
42 of uncultured microbes (Venter et al., 2004; Handelsman, 2004). The rapid expansion of metagenomic
43 datasets presents opportunities and challenges. Metagenomics enables the exploration of complex mi-
44 crobial interactions and genetic evolution of individual species (Xia et al., 2011; Schloissnig et al., 2013).
45 On the other hand, efficient and reliable retrieval of microbial genomes and MGEs from metagenomic
46 sequence pools requires strategic approaches.

47
48 By categorizing metagenomic contigs into distinct groups, the complexity of metagenomes can be re-
49 duced to certain taxonomic levels, from coarse domains to consensus species or strains. Metagenomic
50 applications developed to retrieve intended contigs can be briefly framed into two categories, supervised
51 contig classification tools (i.e., viral contig predictors) and unsupervised contig clustering tools (i.e.,
52 metagenomic binners, see Sedlar et al., 2017 for a review of binning strategies). Viruses are prevalent
53 in aquatic, soil and host-associated systems, and are presumably the most abundant biological entities
54 on Earth (Suttle, 2005, 2007). In marine systems, viral lysis is crucial in redirecting carbon and energy
55 flow to the lower trophic levels (termed “Viral Shunt”), which has great implications for the global
56 biogeochemical cycles (Fuhrman, 1999; Wilhelm & Suttle, 1999). Metagenomic contig classification has
57 been heavily focused on the prediction of viral sequences. VirSorter (Roux et al., 2015) and VirFinder
58 (Ren et al., 2017) are two pioneer tools to identify viral contigs from metagenomic assemblies. VirSorter
59 predicts viral contigs based on viral signals and categorizes them into three tiers with different confi-
60 dence levels. VirFinder employs k-mer frequencies and logistic regression to classify contigs to either
61 viral or host sequences, which outperforms VirSorter at different contig lengths, especially for shorter
62 contigs without detectable viral hallmark genes (Ren et al., 2017). The success of k-mer based methods
63 has inspired the application of deep learning in viral sequence discovery, which led to the development
64 of DeepVirFinder (Ren et al., 2020) and PPR-Meta (Fang et al., 2019), both of which use one-hot encod-
65 ing to convert DNA sequences into presence/absence matrices of nucleotides, and use neural networks
66 to train virus-host classifiers at different contig lengths. Besides, PPR-Meta combines both nucleotide
67 path and codon path in the encoding step, and classifies contigs into viruses, host chromosomes and
68 plasmids (Fang et al., 2019). VIBRANT (Kieft et al., 2020) uses neural networks to distinguish prokary-
69 otic dsDNA, ssDNA and RNA viruses based on “v-score” metrics, which are calculated from significant
70 protein hits to a collection of Hidden Markov Model (HMM) profiles derived from public databases.
71 Most of the aforementioned tools target bacteriophages. Eukaryotic virus predictors are emerging in
72 recent years, and one such tool is HostTaxonPredictor (HTP) (Gałan et al., 2019), which utilizes four
73 machine learning methods to classify viral sequences to eukaryotic viruses or bacteriophages based
74 on sequence features including mono-, dinucleotide absolute frequencies and di-trinucleotide relative

75 frequencies. Plasmids are another major type of MGEs heavily studied in environmental microbiome,
76 particularly in host-associated systems or wastewater treatment plants. Via transferring among hosts
77 or exchanging genes with their host genomes, plasmids facilitate the acquisition of new traits by hosts
78 (Hall, 2016). Thus, by carrying genes related to resource utilization, antibiotic, metal resistance, and
79 defense systems, plasmids contribute to the genetic and phenotypic plasticity of hosts, and increase their
80 fitness to the changing environments. There are multiple dedicated tools developed besides PPR-Meta,
81 such as cBar (Zhou & Xu, 2010), PlasFlow (Krawczyk et al., 2018), PlaScope (Royer et al., 2018) and
82 PlasClass (Pellow et al., 2020). In principle, PlaScope employs a similarity searching approach based on
83 species-specific databases, while cBar, PlasFlow and PlasClass use differential k-mer frequencies with
84 different machine-learning methods. Beyond viruses and plasmids, there is a paucity of applications
85 targeting the classification of eukaryotic contigs from metagenomes, while eukaryotes are indispensable
86 to the ecological functioning of natural microbial communities. Alignment-based applications such as
87 Kaiju (Menzel et al., 2016) and MetaEuk (Levy Karin et al., 2020) search for close matches in reference
88 databases, thus can be used to assign reads or contigs to taxonomic groups. While the accuracy of
89 these applications depends on the completeness of reference databases, their performance in classifying
90 eukaryotic contigs is arguable due to the lack of a comprehensive microbial eukaryotic database (Keel-
91 ing et al., 2014). EukRep (West et al., 2018) is a reference-independent application that uses k-mer
92 frequency and linear-SVM to classify metagenomic contigs into eukaryotic and prokaryotic sequences.
93 It has been proven that when combined with the conventional metagenomic and metatranscriptomic
94 analyses, such as reconstructing eukaryotic bins and gene co-abundance analysis, biological and eco-
95 logical insight can be readily obtained for uncultured eukaryotes (Vorobev et al., 2020; West et al.,
96 2018). Eukaryotic sequences could also be identified using alignment-independent applications. Tiara
97 (Karlicki et al., 2022) is a deep-learning based method used for eukaryotic sequence identification in
98 metagenomes, and Whokaryote (Pronk & Medema, 2022) is a random forest classifier that uses gene-
99 structure based features to distinguish eukaryotic and prokaryotic sequences.

100
101 Despite the significant progress made in the past years, there isn't one tool that can classify eukary-
102 otic/prokaryotic genomes, eukaryotic/prokaryotic viruses, and plasmids in one shot. In fact, all these
103 binary classifiers suffer from sequence types that are not modeled, such as eukaryotic contigs or plasmids
104 can be misclassified as viruses by viral predictors, and viral contigs can be misclassified as plasmids by
105 plasmid predictors, etc. Thus, to achieve a more reliable classification of the target sequences, one has
106 to run several of these tools consecutively, each suffers from its sensitivity and specificity, and the error
107 rates propagate throughout the workflow, resulting in less accurate and biased classification. Here we
108 introduce DeepMicroClass, a versatile multi-class metagenomic contig classifier based on convolutional
109 neural networks (CNN). The implementation of DeepMicroClass and code for experiments described
110 in this paper can be accessed at <https://github.com/chengsly/DeepMicroClass>. We show that
111 DeepMicroClass outperforms all the existing tools by precision and sensitivity across all benchmark
112 datasets with variable sequence-type composition. Using a coastal marine metagenomic dataset as a
113 case study, we showed that DeepMicroClass captures more eukaryotic contigs than alignment-based
114 classifiers. DeepMicroClass is superior to the other tools by classifying all sequence types simultane-
115 ously, which will greatly reduce the time and computation resource usage compared to the conventional
116 workflow of chaining a set of different predictors.

117 Materials and methods

118 Dataset preparation

119 We collected 5 classes of sequences: prokaryotic host, eukaryotic host, plasmid, prokaryotic viral and
120 eukaryotic viral sequences. For prokaryotic chromosome sequences, we downloaded all the prokaryotic
121 genomes, including all the bacteria and archaea sequences from NCBI RefSeq on Aug 22, 2022. The
122 prokaryotic genomes were cleaned up by removing all the sequences annotated as “Plasmid” according
123 to the assembly reports, and sequences not annotated as plasmid but have identical sequence IDs in
124 the plasmid dataset were also removed. The resulting sample set contains 40,208 sequences. The eu-
125 karyotic host sequence database includes eukaryotic sequences from the eukaryotic taxa used by Kaiju
126 (Menzel et al., 2016) and the PR2 database (Guillou et al., 2013). Specifically, we selected microbial
127 eukaryotic genomes under taxa names: “Amoebozoa”, “Apusozoa”, “Cryptophyceae”, “Euglenozoa”,
128 “Stramenopiles”, “Alveolata”, “Rhizaria”, “Haptista”, “Heterolobosea”, “Metamonada”, “Rhodophyta”,
129 “Chlorophyta”, and “Glaucocystophyceae” using genome_updater (available at https://github.com/pirovci/genome_updater) on Aug 22, 2022. A total of 612 eukaryotic sequences were downloaded. In
130 addition to these eukaryotic genomes, we also included 32,073,625 eukaryotic host sequences from the
131 678 marine eukaryotic transcriptomic re-assemblies (Johnson et al., 2019) of cultured samples generated
132 by the MMETSP project (Keeling et al., 2014), which included 306 pelagic and endosymbiotic marine
133 eukaryotic species representing more than 40 phyla.

135

136 Plasmid sequences and corresponding metadata were retrieved from PLSDB (Galata et al., 2019) re-
137 leased on Jun 23, 2021. The dataset contains 34,513 plasmid records. Viral sequences and associated
138 metadata were retrieved from Virus-Host DB (Mihara et al., 2016) released on Jun 1, 2022, which
139 contains 17,357 nucleic acid records, including 5,209 prokaryotic viruses and 12,148 eukaryotic viruses.
140 In all downloaded sequences, we further cross compared sequence IDs in each class, and any sequence
141 with an identical ID occurring in more than one class was removed so that we could reduce potential
142 erroneous annotation from the source database.

143 Benchmark Dataset Preparation

144 Sequences were split into two parts according to the dates submitted to NCBI, using Jan 1, 2020 as a
145 cutoff date. Sequences submitted before Jan 1, 2020 were used for training and validation, with 80%
146 as training and 20% as validation using stratified split, and the sequences submitted after this date
147 were used for testing. The Mash (Ondov et al., 2016) distance was used to estimate the similarity
148 between sequences among training, validation and test sets. Sequences in the test set with a Mash
149 distance < 0.1 to any sequence in the training or validation sets were removed from the test set. Virus-
150 Host DB derived viral sequences (Mihara et al., 2016) and MMETSP derived eukaryotic sequences
151 were not dated. These sequences were randomly split into training, validation and test sets with the
152 proportions of 60%, 20% and 20%, respectively. Similarly, sequences were removed from the test set
153 when the Mash distance < 0.1 to any sequence in the training or validation sets. The composition
154 of a metagenomic sample is usually unknown, and the imbalance among different sequence classes
155 might affect the performance of different classifiers. Moreover, existing methods focus on classifying
156 one special sequence class, e.g. eukaryotic hosts, prokaryotic viruses or plasmids. Some tools could
157 classify two or more sequence classes, for instance, PPR-Meta (Fang et al., 2019) can predict prokaryotic
158 hosts, phages and plasmids. In order to compare with tools developed for a specific sequence class and

159 for multiple sequence classes, we generated 20 equal-sized (1000 contigs, each 10 kbs long) benchmark
160 datasets with a variable composition of the 5 sequence classes. Briefly, the fractions of PROK (including
161 prokaryotic hosts, prokaryotic viruses, and plasmids) to EUK (including eukaryotic hosts and eukaryotic
162 viruses) sequences were determined using the ratios of 9:1, 7:3, 5:5, 3:7, and 1:9. Then for each fixed
163 PROK:EUK ratio, the PROK fraction was further split into prokaryotic hosts, prokaryotic viruses and
164 plasmids based on the ratios of 5:1:1, 4:1:1, 3:1:1, and 2:1:1; and the EUK fraction was further split
165 into eukaryotic hosts and eukaryotic viruses according to the ratio of 5:1, 4:1, 3:1, and 2:1. Finally, the
166 corresponding number of sequences were drawn from the test sequence pool for each class using the
167 ratios specified above, the actual sequence source composition of the 20 test datasets were shown in
168 Fig. S1 and Table S1 in the Supplementary Material.

169 Model Design and Training

170 DeepMicroClass employs a di-path convolutional neural network comprising a base-path and a codon-
171 path to classify input sequences into one of the five classes. For the base-path, the input nucleotide
172 sequence was firstly encoded as a one-hot matrix. Specifically, each of the A, C, G, and T nucleotides
173 was translated into [1, 0, 0, 0], [0, 1, 0, 0], [0, 0, 1, 0], [0, 0, 0, 1], respectively. Any non-ACGT nucleotide
174 was represented with [0, 0, 0, 0]. The reverse complimentary strand of the input sequence can be one-hot
175 encoded simply by flipping the forward one-hot matrix along both row and column. For the codon-path,
176 the forward or reverse base-path matrix was first converted into three 64 dimensional one-hot matrices
177 based on three reading frames, then the three matrices were concatenated into one matrix. Thus, for
178 each strand of a input contig, a di-path incorporating both the base and codon level information was
179 encoded and fed into the following convolutional layers. The overview of the network structure of
180 DeepMicroClass is shown in Fig. 1.

181 The di-path CNN model was trained by minimizing the cross-entropy loss between the predicted class
182 and the actual class of input sequences. The training was run for 3000 epochs with a learning rate
183 of 0.001 and batch size of 256. For each batch, sequences from the whole training dataset were firstly
184 subsampled with weighted random sampling without replacement within an epoch. The weight for
185 samples of each class i was defined as

$$w_i = \frac{\text{number of samples}}{5 \times \text{number of samples in class}_i}$$

186 After the sequences were sampled, a contig length was chosen from 500 bps, 1 kbps, 2 kbps, 3 kbps
187 and 5 kbps, and a contig with the given length was sampled from the original sequence to construct
188 the batch. In the testing stage, sequences with lengths < 5 kbps were fed directly to the model for
189 prediction. For sequences with lengths > 5 kbps, each input sequence was first split into multiple
190 non-overlapping 5 kbps chunks, then scores given by the model for each chunk were collected, and the
191 mean score of all chunks was used as the final output of the input sequence.

192

193 Use-case data preparation and analysis

194 The daily time-series metagenomic samples were taken off the coast of Southern California using an
195 Environmental Sample Processor (ESP), and the 1 μ m A/E filters (Pall Gelman) collected during
196 the day were used for DNA extraction as described previously (Needham et al., 2018). Metagenomic
197 libraries were prepared using the Ovation[®] Ultralow V2 DNA-Seq library preparation kit (NuGEN,

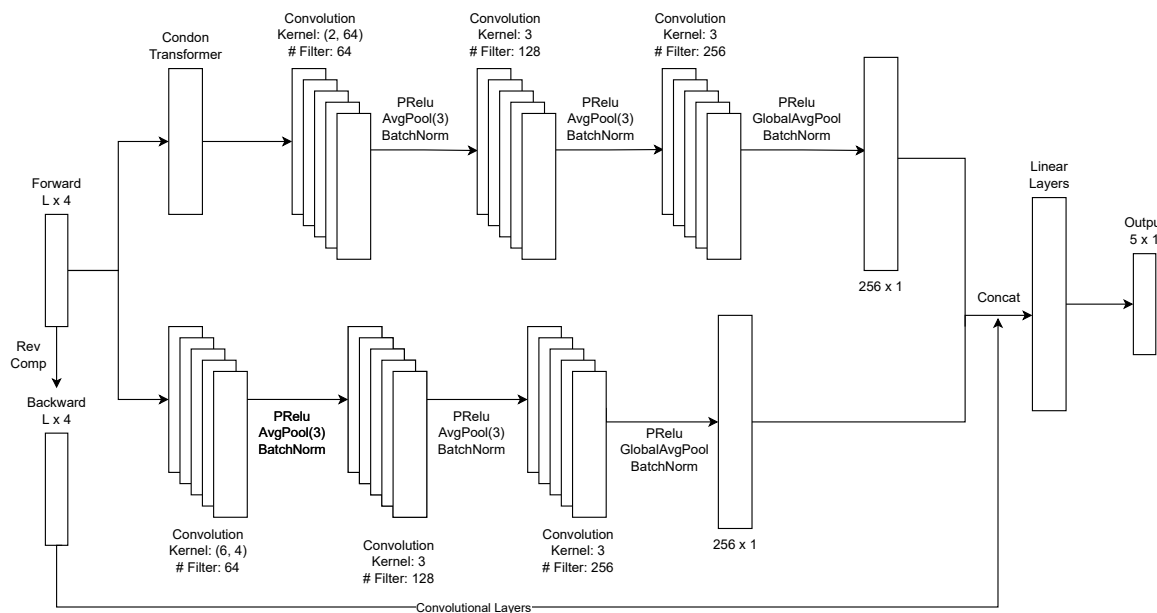


Fig 1. Schematic representation of the multi-class CNN structure used in this study. The network has two convolutional paths, a base-path encodes the nucleotide level information and a codon-path encodes the codon level information. The hyperparameters used for each convolutional layer are marked on the figure. For each strand, the output dimension of base- and codon-paths are 256 and 256, respectively. The di-path outputs of forward and reverse strands are concatenated into a 1024-dimensional vector, which is used as the input of following linear layers. The final linear layer outputs a 5-dimensional vector, with each dimension indicating the probability of the input contig being eukaryotic host, eukaryotic virus, plasmid, prokaryotic host and prokaryotic virus.

198 Tecan Genomics) under the manufacturer's instruction using 10 ng of starting DNA and amplified for
 199 13 PCR cycles. Metagenomic libraries were sequenced on an Illumina NovaSeq 6000 platform (2×150
 200 bp chemistries) at Berry Genomics Co. (Beijing, China). After demultiplexing, the raw reads were
 201 first checked with FastQC v0.11.2, then adapter and low quality regions were trimmed using fastp
 202 v0.21.0 (Chen et al., 2018) with the following parameters: -q 20 -u 20 -l 30 -cut_tail -W 4 -M 20 -c.
 203 PhiX174 and sequencing artifacts were removed using bbdduk.sh and human genome sequences were
 204 removed using bbmap.sh with default parameters, both scripts can be found in the BBTools package
 205 v37.24 (<https://jgi.doe.gov/data-and-tools/bbtools>). Metagenomic samples were assembled indepen-
 206 dently using metaSPAdes v3.13.0 (Nurk et al., 2017) with a custom kmer set (-k 21,33,55,77,99,127).
 207 The assembled contigs were further coassembled as previously described (Long et al., 2021). Briefly,
 208 all the contigs were pooled and sorted into short ($<2\text{kb}$) or long ($\geq 2\text{kb}$) contig sets, the short contig
 209 set was first coassembled using Newbler v2.9 (Margulies et al., 2005), the resulting $\geq 2\text{kb}$ contigs were
 210 further coassembled with the long contig set (Treangen et al., 2011). A minimum overlap thresholds of
 211 80 nt and 200 nt were set for Newbler and minimus2, respectively. For both coassembly steps, a min-
 212 imum identity cutoff of 0.98 was applied. After co-assembly, contigs were further dereplicated at 0.98
 213 identity using cd-hit v4.6.8 (Li & Godzik, 2006), the resulting contigs were used as reference contigs
 214 for sequence classification and read recruitment analysis. Reference contigs were classified using Kaiju
 215 v1.7.3 (Menzel et al., 2016) and MetaEuk v1 (Levy Karin et al., 2020), as well as DeepMicroClass v0.1.0
 216 (in hybrid mode), read counts assigned to each sequence class were summarized using custom Python
 217 scripts. Reads were mapped to reference contigs using bwa mem v0.7.17 with default parameters, and
 218 the number of reads aligned >30 nt to reference contigs were counted using bamcov v0.1 (available at

219 <https://github.com/fbreitwieser/bamcov>) with default parameters.

220 Results

221 A CNN-based multi-class classifier

222 Identifying contigs of microbial eukaryotes and the viruses infecting them from metagenomic assemblies
223 is crucial for gaining a better understanding of their ecological roles. However, current state-of-the-art
224 tools often do not fully appreciate most of the eukaryotic viruses and their hosts. Here two commonly
225 used viral contig predictors, VirFinder (Ren et al., 2017) and PPR-Meta (Fang et al., 2019), were eval-
226 uated based on their predicted viral scores. As expected, both predictors gave high scores to prokaryotic
227 viral sequences and low scores to prokaryotic host sequences. However, the scores for eukaryotic host
228 and eukaryotic viral sequences were more evenly distributed (**Fig. S2**), revealing an insufficient ac-
229 curacy in classifying these sequence classes. Out of 500 randomly subsampled genomic sequences for
230 each sequence type of prokaryotes, prokaryotic viruses, microbial eukaryotes, and eukaryotic viruses
231 downloaded from NCBI, 454 prokaryotic viruses and 85 prokaryotic hosts had VirFinder-scores (VF-
232 scores) above 0.5, while 238 eukaryotic viruses and 157 eukaryotic hosts had VF-scores above this value
233 (**Fig. S2a**). A similar trend can be observed for PPR-Meta (**Fig. S2b**), confirming these tools are
234 not adequately equipped to handle eukaryotic viral and host sequences. This emphasizes the need for
235 novel predictors that consider more sequence types during the model training process.

236 Here the performance of DeepMicroClass on sequences with different lengths (500 bps, 1 kbps, 2 kbps,
237 3 kbps, 5 kbps, 10 kbps, 50 kbps, and 100 kbps) was evaluated on test data. The model performance
238 for each sequence type was visualized via the Receiver Operating Characteristics (ROC) curve using
239 a one-versus-rest strategy (**Fig. 2**). Overall, we showed that as the sequence length increased, the
240 model's performance improved across most sequence types, as indicated by the Area Under the Re-
241 ceiver Operating Characteristic (AUC) measurements (**Fig. 2**). DeepMicroClass performed well on all
242 sequence types when the input sequence length was ≥ 1 kbps, with the minimum AUC score being
243 0.963 on classifying prokaryotic sequences. At the sequence length of 500 bps, DeepMicroClass achieved
244 fairly high AUC scores for eukaryotic (0.944) or prokaryotic (0.96) viruses, whilst the scores for both
245 viral sequence types were always ≥ 0.99 at longer sequence lengths (≥ 2 kbps) (**Fig. 2**). For non-viral
246 sequences, the AUC scores were highest for eukaryotic sequences, followed by plasmid and prokaryotic
247 genome sequences. However, a slight drop in the True Positive Rate (TPR) could be observed for eu-
248 karyotic sequences when the False Positive Rate (FPR) was near 0 (**Fig. 2**). With further investigation,
249 the rough curve could be caused by the sharp drop in the number of available eukaryotic sequences in
250 the training dataset, which dropped from 16,002 to 255 when the contig length changed from 10 kbps
251 to 50 kbps.

253 DeepMicroClass outperforms Tiara and Whokaryote in eukaryotic host sequence 254 prediction

255 In the following three sections, we investigate the performance of DeepMicroClass for particular classes
256 of sequences. We used accuracy and F1 score as the metrics to assess the model performance. And
257 the sequence type composition of different benchmark datasets was described in the section Benchmark
258 Dataset Preparation.

259

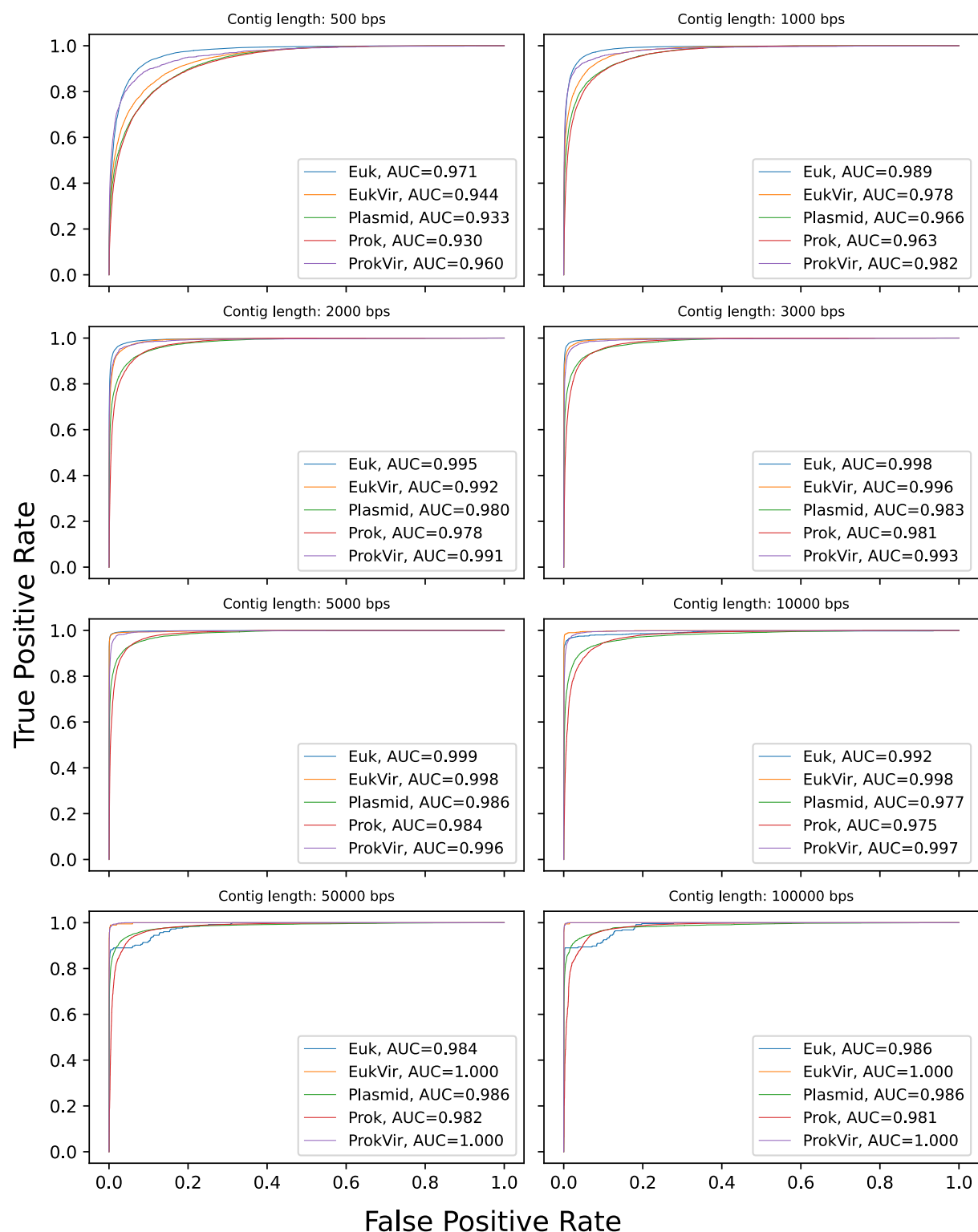


Fig 2. The ROC curves and AUC scores of different length models assessed on test datasets.

Each different panel shows the ROC curves for 5 sequence classes at different contig lengths (500 bps, 1 kbps, 2 kbps, 3 kbps, 5 kbps, 10 kbps, 50 kbps and 100 kbps). Euk, eukaryotic sequences; EukVir, eukaryotic viral sequences; Plasmid, plasmid sequences; Prok, prokaryotic genome sequences; ProkVir, prokaryotic viral sequences.

260 First, we compared the performance of DeepMicroClass with Tiara (Karlicki et al., 2022) and Whokaryote
 261 (Pronk & Medema, 2022) on the classification of microbial eukaryotes. Tiara and Whokaryote are
 262 commonly used to identify eukaryotic contigs from metagenomic assemblies without prior knowledge
 263 of microbial phylogenetic affiliation. With the compiled benchmark datasets, we showed that DeepMi-
 264 croClass persistently outcompeted both tools in all scenarios in terms of accuracy and F1 score (**Fig. 3**,
 265 **S3**), and DeepMicroClass was robust to the different compositions of benchmark datasets (**Fig. 3**).

266

267 The average accuracy and F1 score across all benchmark datasets for DeepMicroClass were both 0.99,
 268 which were significantly higher than these metrics of Tiara and Whokaryote (pairwise Wilcoxon test
 269 p -values $\leq 9.5\text{e-}05$ for both accuracy and F1 score). The accuracy of Whokaryote dropped from ~ 0.95
 270 to ~ 0.75 as the proportion of eukaryotic sequences increased, and the F1 scores were substantially lower
 271 than 0.8 in all test datasets. In contrast, Tiara maintained high accuracy and F1 score across different
 272 eukaryotic proportions, though a slight decrease in accuracy could be observed when the eukaryotic
 273 proportion was high. DeepMicroClass achieved accuracy and F1 score above 0.98 for all tested scenarios
 274 and was robust to variable sequence composition.

275

276 A further look into those misclassified sequences revealed that both Tiara and Whokaryote suffered
 277 from lower sensitivity in distinguishing eukaryotic sequences from other types of sequences. Especially
 278 for Whokaryote, a substantial amount of eukaryotic viruses were mistakenly classified as eukaryotes
 279 (**Fig. S4**).

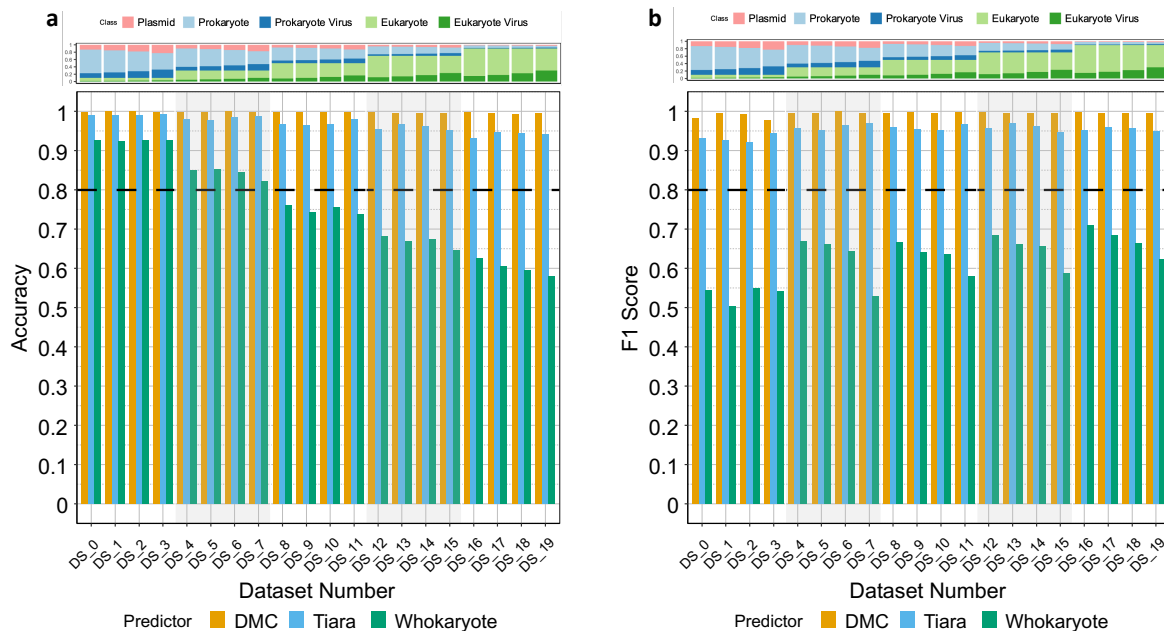


Fig 3. Distribution patterns of accuracy (a) and F1 score (b) across 20 benchmark datasets for DeepMicroClass, Tiara and Whokaryote. The top panel shows the sequence type composition of 20 benchmark datasets, and the detailed composition ratios can be found in Table S1. The dashed black lines indicate where accuracy or F1 score equals 0.8.

280 **DeepMicroClass outcompetes PlasFlow, PPR-Meta and geNomad in plasmid se-
281 quence classification**

282 Plasmids are the major agents of horizontal gene transfer (HGT) among prokaryotic microbial commu-
283 nities. Here we compared the performance of DeepMicroClass with PlasFlow (Krawczyk et al., 2018),
284 PPR-Meta (Fang et al., 2019) and geNomad (Camargo et al., 2023) in classifying plasmid sequences
285 using the same benchmark datasets described above. DeepMicroClass showed significantly improved
286 results than PlasFlow, PPR-Meta and geNomad in all tested cases in plasmid classification (pairwise
287 Wilcoxon test adj.*p*-value $\leq 1.1\text{e-}07$; **Fig. 4 & S5**). Although PlasFlow, PPR-Meta and geNomad were
288 able to achieve a maximum F1 score of 0.68, 0.74 and 0.86, respectively, their performance was severely
289 impaired with increasing proportions of eukaryotic sequences in the benchmark datasets (**Fig. 4**). In
290 contrast, the F1 score of DeepMicroClass was constantly higher than 0.8, though a slight decrease could
291 also be observed with increasing eukaryotic proportions.

292

293 We further examined the misclassified sequences and found PlasFlow had high sensitivity but low
294 specificity, and the dominance of misclassified sequence types was in line with the composition of
295 benchmark datasets (**Fig. S6**). PPR-Meta might benefit from its modeling of prokaryotic chromo-
296 somes and phages, while it still had a low specificity mainly due to the misclassification of prokaryotic
297 and eukaryotic chromosomal sequences into plasmids (**Fig. S6**). On the other hand, geNomad mainly
298 suffered from misclassifying prokaryotic chromosomes into plasmids, though the misclassified eukary-
299 otic sequences also accounted for a significant share (**Fig. S6**). It's noteworthy that DeepMicroClass
300 might further benefit from its modeling of eukaryotic genomic and viral sequences since they were
301 rarely misclassified as plasmids, though the misclassification rates between plasmids and prokaryotic
302 chromosomal sequences were still the highest among all misclassifications (**Fig. S12**). Probable rea-
303 sons for such observation are the high affinity and frequent genetic exchange between plasmids and
304 prokaryotic chromosomes, further improvements on the neural network structures or using additional
305 features extracted from gene- or operon-centric approaches might yield a better classifier.

306 **DeepMicroClass achieves improved results in viral sequence prediction**

307 Viruses are ubiquitously found in every natural system where cellular organisms colonize. Viral con-
308 tigs have been commonly identified from metagenomes or viromes using essentially gene-centric (e.g.
309 VirSorter (Roux et al., 2015), VirSorter2 (Guo et al., 2021), VIBRANT (Kieft et al., 2020)), or
310 oligonucleotide-centric (e.g. VirFinder (Ren et al., 2017), DeepVirFinder (Ren et al., 2020), PPR-Meta
311 (Fang et al., 2019)) approaches, or a combination of both approaches (e.g. geNomad (Camargo et al.,
312 2023)). Here we compared the performance of DeepMicroClass with VirSorter2, geNomad, VIBRANT,
313 DeepVirFinder and PPR-Meta on viral contig prediction using the aforementioned benchmark datasets.
314 Among these methods, DeepVirFinder, VIBRANT, PPR-Meta and geNomad were trained for the pre-
315 diction of prokaryotic viruses, while VirSorter2 was trained for the prediction of both eukaryotic and
316 prokaryotic viruses. We compared the performance of DeepMicroClass with VirSorter2 on the predic-
317 tion of both prokaryotic and eukaryotic viruses, and the performance of DeepMicroClass with other
318 predictors on the prediction of prokaryotic viruses. In either case, DeepMicroClass achieved better
319 performance in terms of both accuracy and F1 score than all the other tested tools (**Fig. 5, S7 & S8**).
320 VIBRANT and VirSorter2 showed slightly lower accuracy than DeepMicroClass, followed by PPR-Meta
321 and DeepVirFinder. More distinct differences were observed in the F1 score metric of these tools across
322 dataset composition, DeepMicroClass achieved an average F1 score of ~ 0.96 , followed by VirSorter2

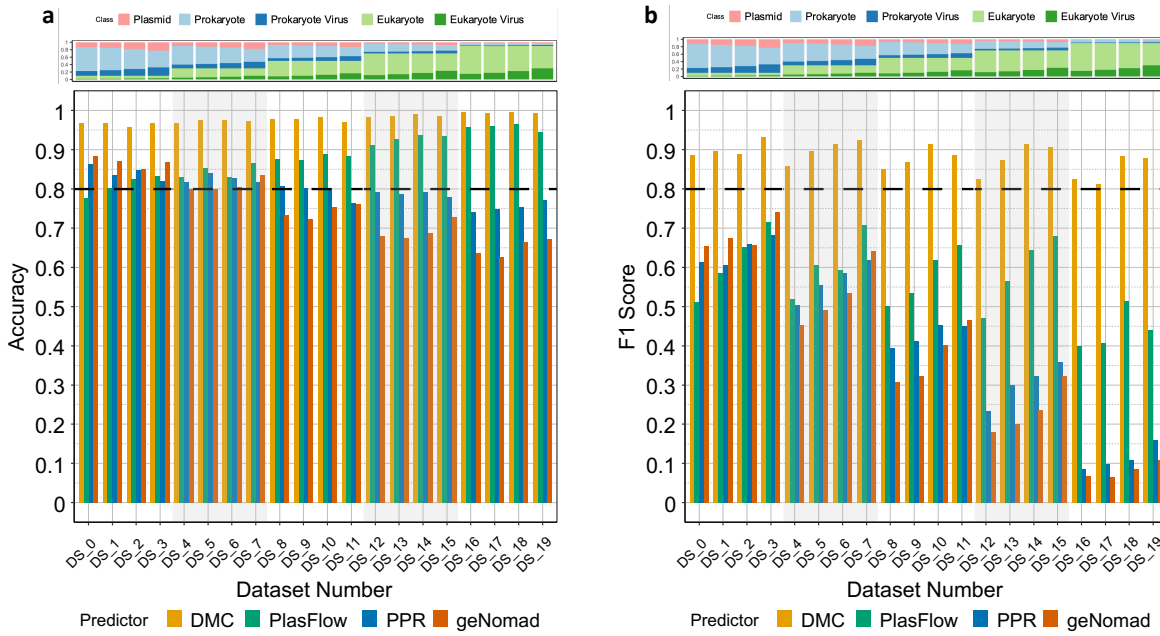


Fig 4. Distribution patterns of accuracy (a) and F1 score (b) across 20 benchmark datasets for DeepMicroClass, PlasFlow, PPR-Meta and geNomad on plasmid classification. The dashed black lines indicate where accuracy or F1 score equals 0.8. The same benchmarking datasets were used as in **Fig. 3**. DMC, DeepMicroClass; PPR, PPR-Meta

323 and VIBRANT (~0.90 and ~0.85, respectively). The F1 score of VIBRANT dropped from 0.94 to <0.80
 324 as increasing proportions of eukaryotic chromosomal and viral sequences in the benchmark datasets.
 325 PPR-Meta and DeepVirFinder showed a decreasing tendency in both accuracy and F1 score with the
 326 increasing of eukaryotic chromosomal and viral sequences (**Fig. 5a & 5b, S7**). When considering both
 327 prokaryotic and eukaryotic viral sequences as the positive viral set, DeepMicroClass and VirSorter2
 328 were both able to achieve accuracy >0.90 and F1 score >0.80 without being significantly affected by
 329 the variations of sequence type composition, and DeepMicroClass constantly outperformed VirSorter2
 330 in both metrics across the benchmark datasets (**Fig. 5c & 5d, S8**).

331

332 The number of misclassified sequences by PPR-Meta, DeepVirFinder, VIBRANT, geNomad and Vir-
 333 Sorter2 is shown in **Fig. S9**. The distribution of misclassified sequences by PPR-Meta, DeepVirFinder
 334 and geNomad showed a similar pattern, that eukaryotic chromosomal and viral sequences were prone
 335 to be misidentified as prokaryotic viruses. This indicates tools or models trained without knowledge
 336 of eukaryotic sequences are likely to behave similarly when eukaryotes are not rare in the metage-
 337 nomic community. Although VIBRANT and VirSorter2 had fewer misclassified sequences compared
 338 to PR-Meta, DeepVirFinder and geNomad, both suffered from misclassifying prokaryotic chromosomal
 339 or plasmid sequences into prokaryotic viruses **Fig. S9**. Since both VIBRANT and VirSorter2 use a
 340 gene-centric approach, it's possible that some of the viral signature genes or fragments could also be
 341 widely detected in prokaryotic genomes or plasmids as a result of frequent gene transfer among them.
 342 This contrasts with the oligonucleotide-centric tools since cross-kingdom viral infection or plasmid con-
 343 jugation and gene transfer are less common.

344

345 Since DeepMicroClass, PPR-Meta and geNomad are multiclass classifiers, here we also compared their
 346 performance based on accuracy and F1 score metrics on multiclass sequence classification using the same

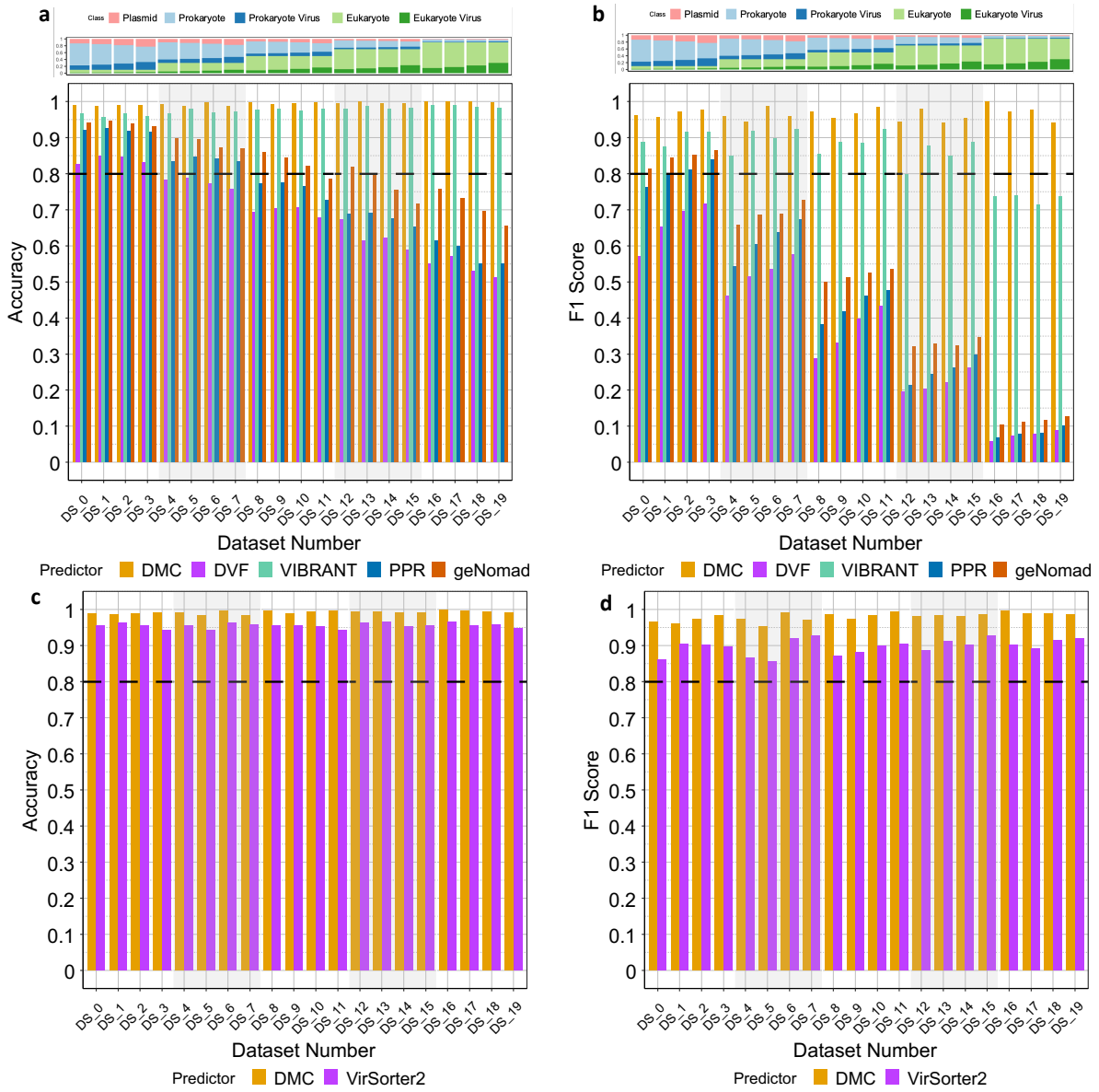


Fig 5. Distribution patterns of accuracy and F1 score across 20 benchmark datasets for viral classification. The accuracy (a) and F1 score (b) metrics for DeepMicroClass, PlasFlow, PPR-Meta and geNomad were evaluated on prokaryotic viral contig classification, and the accuracy (c) and F1 score (d) metrics for DeepMicroClass and VirSorter2 were evaluated on both prokaryotic and eukaryotic viral contig classification. The dashed black lines indicate where accuracy or F1 score equals 0.8. The same benchmark datasets were used as in **Fig. 3**. DMC, DeepMicroClass; DVF, DeepVirFinder; PPR, PPR-Meta.

benchmark datasets (**Fig. S10 & S11**). Here we only considered prokaryotic chromosomal, prokaryotic viral and plasmid sequences for comparison with PPR-Meta and geNomad as they were not trained for eukaryotic sequence classification. On the other hand, all five sequence types were considered for the evaluation of DeepMicroClass. In this case, DeepMicroClass still outperformed PPR-Meta and geNomad in all tested scenarios as evaluated by both the accuracy or and F1 score metrics (pairwise Wilcoxon test p -values $\leq 1.9e-06$; **Fig. S10 & S11**). Both accuracy and F1 scores of DeepMicroClass were rarely below 0.95 across the sequence composition of the 20 benchmark datasets, while they were rarely above 0.9 for geNomad, or rarely above 0.8 for PPR-Meta (**Fig. S10**). Although the performance of DeepMicroClass was also deteriorated by the misclassification between prokaryotic chromosomal and plasmid sequences (**Fig. S12**), the amounts of misclassified sequences were significantly lower than

357 VIBRANT, VirSorter2 or geNomad (**Fig. S9**).

358 **DeepMicroClass predicted more eukaryotic and viral contigs than alignment-based**
359 **predictors**

360 Alignment-based classifiers can suffer from incomplete genomic databases, particularly for complex
361 natural environments such as marine or soil systems. To test the performance of DeepMicroClass in
362 real metagenomic context, here we examined its performance with the other two sequence classifiers,
363 Kaiju (Menzel et al., 2016) and MetaEuk (Levy Karin et al., 2020), using a 1-300 μ m size fraction
364 marine metagenomic dataset sampled off the coast of Southern California (Needham et al., 2018). Us-
365 ing the co-assembled contigs as the reference, we show DeepMicroClass classified less prokaryotic but
366 more eukaryotic, eukaryotic viral and prokaryotic viral contigs than Kaiju and MetaEuk (**Fig. 6a**).
367 Among all the prokaryotic contigs classified by both Kaiju and MetaEuk, 73.6% of them were pre-
368 dicted to be prokaryotic by DeepMicroClass, and 11.88%, 10.39%, and 4.14% of them were predicted
369 to be eukaryotic, prokaryotic viral and eukaryotic viral sequences, respectively (**Fig. 6b**). Contigs that
370 couldn't be taxonomically determined by Kaiju (16.41%) or MetaEuk (10.01%) are mainly dominated
371 by eukaryotic sequences (57.13% / 38.3%) as predicted by DeepMicroClass (**Fig. 6c & 6d**). Although
372 MetaEuk classified more eukaryotic contigs than Kaiju (21.88% vs 15.26%, **Fig. 6a**), the latter clas-
373 sified more prokaryotic viral contigs (4.38% vs 1.51%, **Fig. 6a**). This is consistent with the higher
374 percentage of prokaryotic viral sequences in the unclassified contigs of MetaEuk than Kaiju (28.86%
375 vs 14.87%, **Fig. 6c & 6d**). By mapping reads to reference contigs, we calculated the read percentages
376 recruited by different sequence types. The average eukaryotic read percentage recruited by DeepMi-
377 croClass (6.15%) is considerably higher than by MetaEuk (4.78%) or Kaiju (3.50%), at the expense of
378 lower prokaryotic read percentages (13.12%, 20.60% and 20.51%, respectively, **Fig. 6f-h**). Similarly,
379 the average read percentages of prokaryotic viral and eukaryotic viral sequences recruited by Deep-
380 MicroClass (6.07%/1.24%) are also higher than MetaEuk (0.49%/0.19%) and Kaiju (1.67%/0.37%)
381 (**Fig. 6f-h**). Notably, though DeepMicroClass assigned less prokaryotic and more eukaryotic reads
382 than other classifiers, the relative abundance profiles across the whole time series are highly correlated
383 (**Fig. S13a & S13b**), and to a less extent for the prokaryotic viral read percentage profiles (**Fig.**
384 **S13c**). This is not the case for eukaryotic viral read abundance profiles, where Kaiju and MetaEuk
385 are highly correlated, but not to DeepMicroClass (**Fig. S13d**). To sum up, DeepMicroClass is more
386 correlated with MetaEuk in eukaryotic read profiles, and more correlated with Kaiju in prokaryotic
387 and prokaryotic viral read profiles.

388 **Discussion**

389 **Microbial eukaryotes and viruses infecting them are understudied**

390 Microbial eukaryotes are prevalent in diverse ecosystems such as host-associated habitats (Parfrey et al.,
391 2011), deep-sea benthos (Bik et al., 2012), and geothermal springs (Oliverio et al., 2018), etc. Due to
392 challenges in the cultivation and whole genome-sequencing of microbial eukaryotes, biodiversity sur-
393 veys of microbial eukaryotes were commonly performed using marker genes, such as the 18S rDNA
394 hypervariable V4 or V9 regions (Pawlowski et al., 2012; Amaral-Zettler et al., 2009). The amplicon-
395 based analysis provides valuable information on the taxonomy of microbial eukaryotes, while in order
396 to probe their metabolic potentials or ecological functions, genomic and transcriptomic information
397 are essential. Despite several achievements in collecting microbial eukaryotic genes (Carradec et al.,

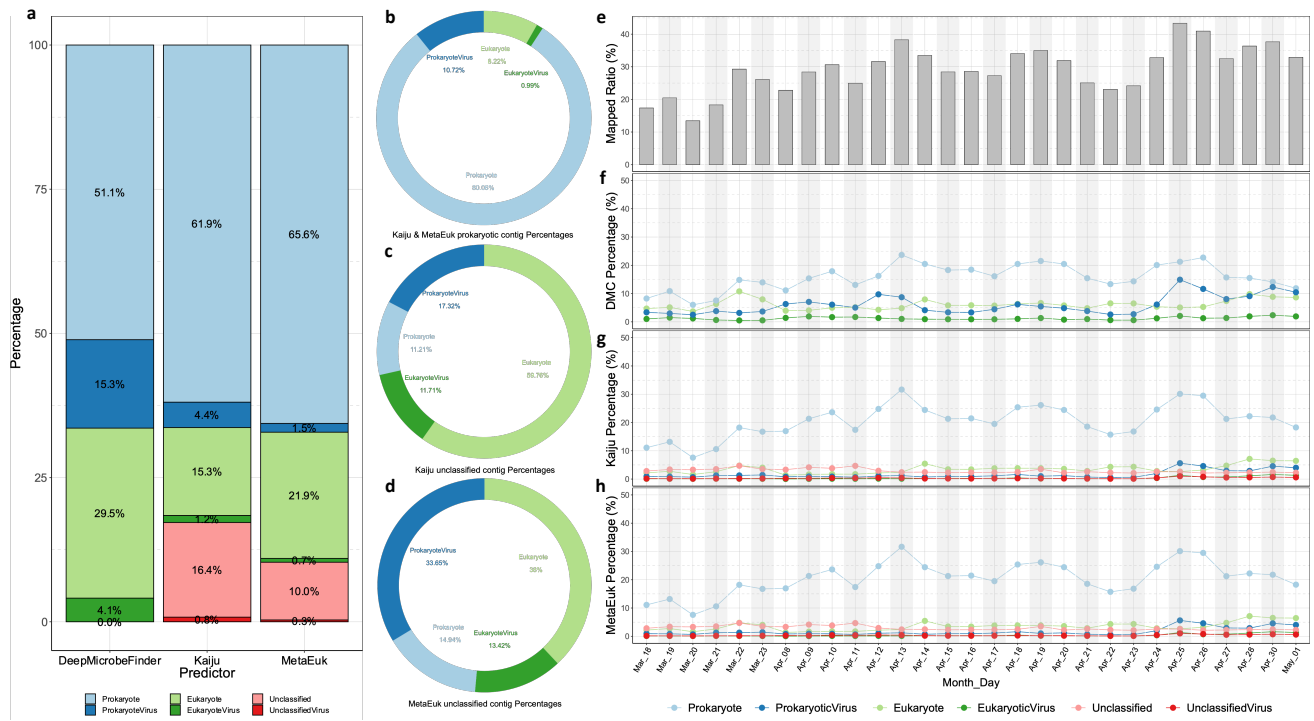


Fig 6. Sequence classification and read abundance of a 1-300 μm size fraction marine metagenomic dataset sampled off the coast of Southern California. Metagenomic contigs were classified using DeepMicroClass, Kaiju and MetaEuk at a length cutoff of 2 kb, and percentages of different sequence types were calculated (a). Contigs predicted as Prokaryotes by both Kaiju and MetaEuk (b), and contigs that were not classified by Kaiju (c) or MetaEuk (d) were further broken down into DeepMicroClass's classification. Clean reads were aligned to metagenomic contigs and percentages of mappable reads were calculated (e). Mapped read percentages were further summarized according to sequence types of reference contigs as predicted by DeepMicroClass (f), Kaiju (g) and MetaEuk (h). Prokaryotes included both prokaryotic hosts and plasmids. UnclassifiedViruses were sequences predicted to be viruses but their taxonomy couldn't be further resolved by Kaiju or MetaEuk.

398 2018; Vorobev et al., 2020), transcripts (Keeling et al., 2014) or single-cell amplified genomes (SAGs)
399 (Sieracki et al., 2019) towards a comprehensive microbial eukaryotic database, our knowledge are still
400 limited by the availability of diverse microbial eukaryotic genomes (Burki et al., 2020). With the rapid
401 accumulation of metagenomic datasets and the availability of binning software, it's appealing to recover
402 eukaryotic genomes from natural microbial communities. EukRep was developed in such a context to
403 identify eukaryotic contigs for metagenomic binning (West et al., 2018). This approach has enabled the
404 genome-resolved analysis of fungi, protists, and rotifers from human microbiome studies (West et al.,
405 2018; Olm et al., 2019). Similar approaches have been applied to marine microbiome studies (Duncan
406 et al., 2020; Delmont et al., 2020), which recovered hundreds of eukaryotic metagenome-assembled
407 genomes (MAGs) and provided insight into the functional diversity and evolutionary histories of micro-
408 bial eukaryotes beyond the taxonomic information.

409
410 Beyond microbial eukaryotes, current viromic studies are biased towards viruses infecting prokaryotes.
411 This could be introduced by the skewed distribution of viral genomes in the RefSeq database, which
412 is dominated by phages and pathogenic viruses. By Sept 1, 2023, among 18,729 viral reference se-
413 quences, there were only 104 records belonging to algae-infecting Phycodnaviridae and 30 belonging to
414 protists-infecting Mimiviridae. Both of the two viral families are subgroups of the Nucleocytoplasmic
415 Large DNA Viruses (NCLDV) (Iyer et al., 2001). Since most of the commonly used viral predictors are

416 trained on the RefSeq viral database, it's expected that these tools suffered from identifying eukaryotic
417 viruses from the test datasets (**Fig. 5, S7, & S8**). Given the high diversity of protists (Foissner, 1999;
418 Slapeta et al., 2005), high throughput metagenomes and single-cell genomes are expected to offer a
419 culture-independent solution to rapidly expand the coverage of viral database. For instance, two recent
420 studies reconstructed 2,074 and 501 NCLDV MAGs from global environmental metagenomes (Schulz
421 et al., 2020; Moniruzzaman et al., 2020), dramatically increased the phylogenetic and functional di-
422 versity of NCLDVs. Single-cell metagenomics was also employed to identify viruses infecting marine
423 microbial eukaryotes (Needham et al., 2019a,b), these studies provided insightful findings of the viral
424 encoded proteins and metabolic pathways.

425
426 These studies demonstrated that metagenomics and single-cell genomics can be promising in studying
427 microbial eukaryotes and viruses infecting them. While most commonly used tools are not optimized in
428 classifying eukaryotes (**Fig. 3 & S3**) or eukaryotic viruses (**Fig. 5 & S7**). Given the high performance
429 of DeepMicroClass and the evidence of abundant eukaryotic contigs in marine ecosystems (**Fig. 6**), we
430 expect it will be a valuable addition to the toolbox of marine ecologists.

431 The challenge of classifying prokaryotic host and plasmid sequences

432 DeepMicroClass has a relatively lower accuracy in classifying plasmids when compared to the classifica-
433 tion of eukaryotic or viral contigs (**Fig. 3, 4, 5**). The majority of the sequences that were misclassified
434 as plasmids were from prokaryotic host genomes (**Fig. S12**), confirming classifying prokaryotic chromo-
435 somal and plasmid sequences is a caveat of DeepMicroClass (**Fig. 2**). In comparison, the other tested
436 plasmid classifiers suffered from both prokaryotic and eukaryotic sequences as we have benchmarked
437 (**Fig. 4 & S6**). It's noteworthy that this marginal advantage can be crucial in natural environments,
438 such as marine environments as we mentioned here (**Fig. 6**), where eukaryotic sequences can have a
439 substantial impact on the classification of plasmid sequences. This also indicates that it is achievable
440 to separate plasmid sequences from eukaryotic sequences solely based on patterns of oligonucleotides,
441 and current plasmid predictors can benefit from using a more comprehensive training dataset including
442 eukaryotic sequences.

443
444 It is understandable given the higher genome complexity of eukaryotes than prokaryotes (Lynch & Con-
445 ery, 2003), such as the coding density, prevalence of introns and repetitive sequences, etc. In contrast,
446 it's challenging to classify plasmids and prokaryotic chromosomal sequences for all the tested plasmid
447 predictors (**Fig. 4**). The reasons can be manifold, but plasmid transmission among microbial hosts
448 and plasmid-chromosome gene shuffling can be two fundamental ones. The host range of plasmids is
449 variable, it can be within closely related species for narrow host range plasmids or across distant phylo-
450 genetic groups for broad host range plasmids (Jain & Srivastava, 2013). Broad host range plasmids can
451 be important drivers of the gene flux among host microbes in natural environments (Heuer & Smalla,
452 2007; Wolska, 2003; Davison, 1999). For instance, in natural soil microbial communities, the IncP-
453 and IncPromA-type broad host range plasmids could transfer from proteobacteria to diverse bacteria
454 belonging to 11 bacterial phyla (Klümper et al., 2015). When plasmid carriage could increase the
455 hosts' fitness, such as improving host survival with antibiotic resistance, it can be rapidly adopted and
456 persistently maintained in natural microbial communities (Li et al., 2020; Bellanger et al., 2014). On
457 the other hand, when the maintenance of plasmids imposed a high fitness cost on the hosts, plasmids
458 or plasmid-borne genes could be lost in the process of purifying selection (Hall et al., 2016). Interest-

459 ingley, studies also suggested that sometimes this fitness cost could be ameliorated by compensatory
460 evolution (Millan et al., 2014; Harrison et al., 2015; Loftie-Eaton et al., 2017), which was hypothesized
461 to be the major factor of plasmid survival and persistence (Hall et al., 2017). Plasmid carriage also
462 increases the chance of plasmid-chromosome genetic exchange mediated by SOS-induced mutagenesis
463 (Rodríguez-Beltrán et al., 2021) or mobile genetic elements such as transposons and integrons, etc
464 (Frost et al., 2005; Rodríguez-Beltrán et al., 2021). For instance, genes carried by transposons or in
465 the variable regions were also frequently found on plasmids (Eberhard, 1990; Zheng et al., 2015). Thus,
466 the permissive transfer of plasmids across diverse hosts and the plasmid-chromosome gene flow pose a
467 challenge for current plasmid classifiers. The oligonucleotide-based approaches might be complemented
468 by gene-centric approaches using plasmid signature genes or enriched gene functions, such as genes
469 involved in mobilization or conjugation. In addition, a comprehensive plasmid database is also crucial
470 for model training, and plasmid-enriched metagenomics (plasmidome) can be a promising way to screen
471 plasmids from environmental samples (Shi et al., 2018).

472

473 **Conclusions**

474 DeepMicroClass as a versatile multi-class classifier enables the accurate classification of five different
475 metagenomic sequence types in one shot, meanwhile, it avoids the time-consuming and error-prone
476 preprocessing steps that could potentially propagate errors to the final classification. The inclusive
477 modeling of all common sequence types in metagenomes also makes DeepMicroClass attain better per-
478 formance than the other state-of-the-art individual predictors due to reduced cross misclassifications.
479 We also detected high relative abundances of marine eukaryotes in a daily time-series dataset, which
480 were underestimated by alignment-based classifiers due to the limitation of public reference databases.
481 Our case study indicates that both host and viral sequences are essential components in the cellular
482 metagenomes, and robust ecological patterns can be obtained with DeepMicroClass even for coarse
483 sequence types. We argue that by using DeepMicroClass as a preliminary classification step on metage-
484 nomic/viromic assemblies, one can further focus on the interested sequence types for the following
485 analysis, such as metagenomic binning of prokaryotic or eukaryotic contigs, comparative genomic anal-
486 ysis of viral or plasmid sequences, etc. We conclude DeepMicroClass achieves higher performance
487 than the other benchmarked predictors, and its application can facilitate studies of under-appreciated
488 sequence types, such as microbial eukaryotic or viral sequences.

489 **Availability of data and materials**

490 The source code and user guide are available at <https://github.com/chengsly/DeepMicrobeFinder>.
491 Benchmark datasets have been deposited at figshare (available at [dx.doi.org/10.6084/m9.figshare.14576193](https://doi.org/10.6084/m9.figshare.14576193)).
492 Raw reads for the case study were deposited at NCBI under the umbrella bioproject PRJNA739254.
493 Additional details of data and analysis are available from the corresponding authors upon request.

494 **Competing interests**

495 The authors declare that they have no competing interests.

496 **Authors' contributions**

497 SH, JAF, and FS conceived the project; SH, TT, SC and FS designed the neural network structure and
498 model evaluation procedures; SH and TT designed the training, test datasets and use-case applications;
499 SH, TT and SC prepared the training and test datasets; TT, SC and SH implemented the software
500 and performed the data analysis; SH, TT and SC prepared all the figures and tables; SH drafted the
501 manuscript; TT, SC, TC, JAF and FS reviewed and edited the manuscript.

502 **Acknowledgements**

503 This study was supported by the NIH grant (Grant ID: 2125142) to F. Sun, the Simons Collaboration on
504 Computational Biogeochemical Modeling of Marine Ecosystems/CBIOMES) grant (Grant ID: 549943)
505 and the Gordon and Betty Moore Foundation (Grant Number: 3779) to J. Fuhrman, the NSFC grants
506 to S. Hou (Grant ID: 42276163) and T. Chen (Grant ID: 61872218, 61721003), the Shenzhen Science,
507 Technology and Innovation Commission Programme to S. Hou (Grant ID: JCYJ20220530115401003),
508 and the National Key R&D Program of China (Grant ID: 2019YFB1404804) to T. Chen. The funders
509 had no roles in study design, data collection or analysis, the decision to publish, and the preparation of
510 the manuscript. We thank Dr. David M. Needham, Dr. J. Cesar Ignacio-Espinoza, and Erin B. Fichot
511 for their help with DNA extraction and metagenomic library preparation.

512 **List of abbreviations**

513 Abbreviations used in this manuscript:

| Abbreviations | Definition |
|---------------|--------------------------------------|
| CEOs | capsid-encoding organisms |
| REOs | ribosome-encoding cellular organisms |
| MGEs | mobile genetic elements |
| SSU rRNA | small subunit ribosomal RNA |
| HMM | hidden Markov model |
| CNN | convolutional neural network |
| ESP | environmental sample processor |
| ROC | receiver operating characteristics |
| AUC | area under the ROC curve |
| TPR | true positive rate |
| FPR | false positive rate |
| HGT | horizontal gene transfer |
| SAGs | single-cell amplified genomes |
| MAGs | metagenome-assembled genomes |
| NCLDV | nucleocytoplasmic large DNA viruses |

514

515 **Supporting information**

516 **Supplemental Table S1. The composition of 20 benchmark datasets used in this study.**
517 PROK includes prokaryotic genomes, plasmids and prokaryotic viruses; EUK includes eukaryotic

518 genomes and viruses. Prok: prokaryotic genomes, ProkVir: prokaryotic viruses/phages, Plas-
519 mids, Euk: eukaryotic genomes, EukVir: eukaryotic viruses. Benchmark sequence files can be found at
520 dx.doi.org/10.6084/m9.figshare.14576193.

521 **Supplemental Figure S1. Sequence source composition of 20 equal-sized benchmark datasets.**
522 The fractions of PROK (including prokaryotic hosts, prokaryotic viruses, and plasmids) to EUK (in-
523 cluding eukaryotic hosts and eukaryotic viruses) sequences were determined using the ratios of 9:1, 7:3,
524 5:5, 3:7, and 1:9. For each fixed PROK:EUK ratio, the PROK fraction was further split into prokary-
525 otic hosts, prokaryotic viruses and plasmids based on the ratios of 5:1:1, 4:1:1, 3:1:1, and 2:1:1; and the
526 EUK fraction was further split into eukaryotic hosts and eukaryotic viruses according to the ratio of
527 5:1, 4:1, 3:1, and 2:1. The detailed ratios can be found in Table S1.

528 **Supplemental Figure S2. The distribution of viral confidence scores for (a) VirFinder and**
529 **(b) PPR-Meta. For both predictors, the same dataset was used and the predictions were**
530 **performed with default parameters.** VirFinder uses VF-Scores to determine the likelihood of input
531 sequences being viral or not, and PPR-Meta uses phage scores to discern viruses from host chromosomes
532 and plasmids. Both predictors achieved a high recall for prokaryotic viruses, while the confidence scores
533 of eukaryotic viruses were more evenly spread across all confidence regions. Besides, both predictors
534 achieved a high performance in distinguishing prokaryotic host sequences from prokaryotic viruses, but
535 less so for eukaryotic host sequences.

536 **Supplemental Figure S3. Performance of DeepMicroClass, Tiara and Whokaryote on**
537 **eukaryotic sequence classification.** Both the accuracy and F1 score were compared based on 20
538 designed benchmark datasets. The sequence class composition of the 20 datasets can be found in Table
539 S1. Values on top of the pairwise comparisons are Bonferroni adjusted t-test *p*-values. The significance
540 of the overall ANOVA test was shown in the bottom left corner.

541 **Supplemental Figure S4. The distribution of misclassified sequence types by Tiara and**
542 **Whokaryote.** The distribution of misclassified sequence types by Tiara and Whokaryote. The se-
543 quence composition of these datasets can be found in Table Supplemental Table S1. To make the figure
544 more visible, the range of the *y*-axis is from 0 to 100 for Tiara and from 0 to 500 for Whokaryote.

545 **Supplemental Figure S5. Performance of DeepMicroClass, PlasFlow, PPR-Meta and**
546 **geNomad on plasmid sequence classification.** Both the accuracy and F1 score were compared
547 based on 20 designed benchmark datasets. The sequence class composition of the datasets can be found
548 in Table S1. Values on top of the pairwise comparisons are Bonferroni-adjusted t-test *p*-values. The
549 significance of the overall ANOVA test is shown in the bottom left corner.

550 **Supplemental Figure S6. The distribution of misclassified sequence types by PlasFlow,**
551 **PPR-Meta and geNomad.** The sequence composition of these datasets can be found in Table S1.

552 **Supplemental Figure S7. Performance of DeepMicroClass (DMC), DeepVirFinder (DVF),**
553 **VIBRANT, PPR-Meta (PPR) and geNomad on prokaryotic viral sequence classification.**
554 Both the accuracy and F1 score were compared based on 20 designed benchmark datasets. The sequence

555 class composition of the 20 test datasets can be found in Table S1. Values on top of the pairwise com-
556 parisons are Bonferroni-adjusted t-test *p*-values. The significance of the overall ANOVA test is shown
557 in the bottom left corner

558 **Supplemental Figure S8. Performance of DeepMicroClass and VirSorter2 on prokaryotic**
559 **and eukaryotic viral sequence classification.** Both the accuracy and F1 score were compared based
560 on 20 designed benchmark datasets. The sequence class composition of these datasets can be found
561 in Table S1. Values on top of the pairwise comparisons are Bonferroni-adjusted t-test *p*-values. The
562 significance of the overall ANOVA test is shown in the bottom left corner.

563 **Supplemental Figure S9. The distribution of misclassified sequence types by PPR-Meta,**
564 **DeepVirFinder, VIBRANT, geNomad and VirSorter2.** For PPR-Meta, DeepVirFinder, VI-
565 BRANT and geNomad, only prokaryotic viruses are considered as the positive set, and for VirSorter2
566 both prokaryotic and eukaryotic viruses are considered positive. The sequence composition of these
567 datasets can be found in Table S1. To make the figure more visible, the range of the *y*-axis is from 0 to
568 500 for PPR-Meta and DeepVirFinder, from 0 to 50 for VIBRANT, and from 0 to 80 for VirSorter2.

569 **Supplemental Figure S10. Distribution patterns of accuracy (a) and F1 score (b) across**
570 **20 benchmark datasets for DeepMicroClass, PPR-Meta and geNomad on the prokaryotic**
571 **genome, prokaryotic virus and plasmid classification.** DeepMicroClass received higher scores
572 in both accuracy and F1 score metrics in all tested scenarios compared to PPR-Meta and geNomad in
573 multi-class classification. The dashed black lines indicate where accuracy or F1 score equals 0.8. The
574 same benchmark datasets were used as in Fig. **Fig. 3.**

575 **Supplemental Figure S11. Performance of DeepMicroClass, PPR-Meta and geNomad on**
576 **the prokaryotic genome, prokaryotic virus and plasmid classification.** Both the accuracy and
577 F1 score were compared based on 20 designed benchmark datasets. The sequence class composition of
578 these datasets can be found in Table S1. Values on top of the pairwise comparisons are Bonferroni-
579 adjusted t-test *p*-values. The significance of the overall ANOVA test is shown in the bottom left corner.

580 **Supplemental Figure S12. The distribution of misclassified sequence types by DeepMi-**
581 **croClass.** The sequence composition of these datasets can be found in Table S1. The maximal number
582 of errors across all benchmark datasets was 50, which was set as the maximum of the *y*-axis.

583 **Supplemental Figure S13. Correlation coefficients of Prokaryotic (a), Eukaryotic (b),**
584 **ProkaryoticViral (c), and EukaryoticViral (d) sequence relative abundances of different**
585 **sequence classifiers.** Coefficients highlighted in colors are significant ones (*p*-value < 0.01).

References

Amaral-Zettler, L. A., McCliment, E. A., Ducklow, H. W., & Huse, S. M. (2009). A method for studying protistan diversity using massively parallel sequencing of v9 hypervariable regions of small-subunit ribosomal rna genes. *PLOS ONE*, 4(7), e6372.

Azam, F., & Worden, A. Z. (2004). Oceanography. microbes, molecules, and marine ecosystems. *Science (New York, N.Y.)*, 303(5664), 1622–1624.

Bellanger, X., Guilloteau, H., Breuil, B., & Merlin, C. (2014). Natural microbial communities supporting the transfer of the incP-1 plasmid pb10 exhibit a higher initial content of plasmids from the same incompatibility group. *Frontiers in Microbiology*, 0.

URL <https://www.frontiersin.org/articles/10.3389/fmicb.2014.00637/full>

Bik, H. M., Sung, W., Ley, P. D., Baldwin, J. G., Sharma, J., Rocha-Olivares, A., & Thomas, W. K. (2012). Metagenetic community analysis of microbial eukaryotes illuminates biogeographic patterns in deep-sea and shallow water sediments. *Molecular Ecology*, 21(5), 1048–1059.

Burki, F., Roger, A. J., Brown, M. W., & Simpson, A. G. B. (2020). The new tree of eukaryotes. *Trends in Ecology & Evolution*, 35(1), 43–55.

Béjà, O., Suzuki, M. T., Koonin, E. V., Aravind, L., Hadd, A., Nguyen, L. P., Villacorta, R., Amjadi, M., Garrigues, C., Jovanovich, S. B., & et al. (2000). Construction and analysis of bacterial artificial chromosome libraries from a marine microbial assemblage. *Environmental Microbiology*, 2(5), 516–529.

Camargo, A. P., Roux, S., Schulz, F., Babinski, M., Xu, Y., Hu, B., Chain, P. S., Nayfach, S., & Kyrpides, N. C. (2023). You can move, but you can't hide: identification of mobile genetic elements with genomad. *bioRxiv*, (pp. 2023–03).

Carradec, Q., Pelletier, E., Da Silva, C., Alberti, A., Seeleuthner, Y., Blanc-Mathieu, R., Lima-Mendez, G., Rocha, F., Tirichine, L., Labadie, K., & et al. (2018). A global ocean atlas of eukaryotic genes. *Nature Communications*, 9(11), 373.

Chen, S., Zhou, Y., Chen, Y., & Gu, J. (2018). fastp: an ultra-fast all-in-one fastq preprocessor. *Bioinformatics (Oxford, England)*, 34(17), i884–i890.

Davison, J. (1999). Genetic exchange between bacteria in the environment. *Plasmid*, 42(2), 73–91.

Delmont, T. O., Gaia, M., Hinsinger, D. D., Fremont, P., Guerra, A. F., Eren, A. M., Vanni, C., Kourlaiev, A., d'Agata, L., Clayssen, Q., & et al. (2020). Functional repertoire convergence of distantly related eukaryotic plankton lineages revealed by genome-resolved metagenomics. *bioRxiv*, (p. 2020.10.15.341214).

Duncan, A., Barry, K., Daum, C., Eloe-Fadrosh, E., Roux, S., Tringe, S. G., Schmidt, K., Valentin, K. U., Varghese, N., Grigoriev, I. V., & et al. (2020). Metagenome-assembled genomes of phytoplankton communities across the arctic circle. *bioRxiv*, (p. 2020.06.16.154583).

Eberhard, W. G. (1990). Evolution in bacterial plasmids and levels of selection. *The Quarterly Review of Biology*, 65(1), 3–22.

Falkowski, P. G., Fenchel, T., & Delong, E. F. (2008). The microbial engines that drive earth's biogeochemical cycles. *Science*, 320(5879), 1034–1039.

Fang, Z., Tan, J., Wu, S., Li, M., Xu, C., Xie, Z., & Zhu, H. (2019). Ppr-meta: a tool for identifying phages and plasmids from metagenomic fragments using deep learning. *GigaScience*, 8(6).

URL <https://www.ncbi.nlm.nih.gov/pmc/articles/PMC6586199/>

Foissner, W. (1999). Protist diversity: estimates of the near-imponderable. *Protist*, 150(4), 363–368.

Frost, L. S., Leplae, R., Summers, A. O., & Toussaint, A. (2005). Mobile genetic elements: the agents of open source evolution. *Nature Reviews Microbiology*, 3(9), 722–732.

Fuhrman, J. A. (1999). Marine viruses and their biogeochemical and ecological effects. *Nature*, 399(6736), 541–548.

Galata, V., Fehlmann, T., Backes, C., & Keller, A. (2019). Plsdb: a resource of complete bacterial plasmids. *Nucleic Acids Research*, 47(D1), D195–D202.

Gałan, W., Bąk, M., & Jakubowska, M. (2019). Host taxon predictor - a tool for predicting taxon of the host of a newly discovered virus. *Scientific Reports*, 9(1), 3436.

Guillou, L., Bachar, D., Audic, S., Bass, D., Berney, C., Bittner, L., Boutte, C., Burgaud, G., de Vargas, C., Decelle, J., & et al. (2013). The protist ribosomal reference database (pr2): a catalog of unicellular eukaryote small sub-unit rrna sequences with curated taxonomy. *Nucleic Acids Research*, 41(D1), D597–D604.

Guo, J., Bolduc, B., Zayed, A. A., Varsani, A., Dominguez-Huerta, G., Delmont, T. O., Pratama, A. A., Gazitúa, M. C., Vik, D., Sullivan, M. B., & Roux, S. (2021). Virsorter2: a multi-classifier, expert-guided approach to detect diverse dna and rna viruses. *Microbiome*, 9(1), 37.

Hall, J. P. J., Brockhurst, M. A., Dytham, C., & Harrison, E. (2017). The evolution of plasmid stability: Are infectious transmission and compensatory evolution competing evolutionary trajectories? *Plasmid*, 91, 90–95.

Hall, J. P. J., Wood, A. J., Harrison, E., & Brockhurst, M. A. (2016). Source-sink plasmid transfer dynamics maintain gene mobility in soil bacterial communities. *Proceedings of the National Academy of Sciences of the United States of America*, 113(29), 8260–8265.

Hall, W. A. H. E. B. M., J. (2016). Source-sink plasmid transfer dynamics maintain gene mobility in soil bacterial communities. *Proc. Natl. Acad. Sci. U.S.A.*, 113, 8260–8265.

Handelsman, J. (2004). Metagenomics: application of genomics to uncultured microorganisms. *Microbiology and molecular biology reviews: MMBR*, 68(4), 669–685.

Harrison, E., Guymer, D., Spiers, A. J., Paterson, S., & Brockhurst, M. A. (2015). Parallel compensatory evolution stabilizes plasmids across the parasitism-mutualism continuum. *Current biology: CB*, 25(15), 2034–2039.

Heuer, H., & Smalla, K. (2007). Horizontal gene transfer between bacteria. *Environmental Biosafety Research*, 6(1–2), 3–13.

Iyer, L. M., Aravind, L., & Koonin, E. V. (2001). Common origin of four diverse families of large eukaryotic dna viruses. *Journal of Virology*, 75(23), 11720–11734.

Jain, A., & Srivastava, P. (2013). Broad host range plasmids. *FEMS Microbiology Letters*, 348(2), 87–96.

Johnson, L. K., Alexander, H., & Brown, C. T. (2019). Re-assembly, quality evaluation, and annotation of 678 microbial eukaryotic reference transcriptomes. *GigaScience*, 8(4).

URL <https://doi.org/10.1093/gigascience/giy158>

Karlicki, M., Antonowicz, S., & Karnkowska, A. (2022). Tiara: deep learning-based classification system for eukaryotic sequences. *Bioinformatics*, 38(2), 344–350.

Keeling, P. J., Burki, F., Wilcox, H. M., Allam, B., Allen, E. E., Amaral-Zettler, L. A., Armbrust, E. V., Archibald, J. M., Bharti, A. K., Bell, C. J., & et al. (2014). The marine microbial eukaryote transcriptome sequencing project (mmetsp): Illuminating the functional diversity of eukaryotic life in the oceans through transcriptome sequencing. *PLOS Biology*, 12(6), e1001889.

Kieft, K., Zhou, Z., & Anantharaman, K. (2020). Vibrant: automated recovery, annotation and curation of microbial viruses, and evaluation of viral community function from genomic sequences. *Microbiome*, 8(1), 90.

Klümper, U., Riber, L., Dechesne, A., Sannazzaro, A., Hansen, L. H., Sørensen, S. J., & Smets, B. F. (2015). Broad host range plasmids can invade an unexpectedly diverse fraction of a soil bacterial community. *The ISME Journal*, 9(4), 934–945.

Krawczyk, P. S., Lipinski, L., & Dziembowski, A. (2018). Plasflow: predicting plasmid sequences in metagenomic data using genome signatures. *Nucleic Acids Research*, 46(6), e35–e35.

Legault, B. A., Lopez-Lopez, A., Alba-Casado, J. C., Doolittle, W. F., Bolhuis, H., Rodriguez-Valera, F., & Papke, R. T. (2006). Environmental genomics of “haloquadratum walsbyi” in a saltern crystallizer indicates a large pool of accessory genes in an otherwise coherent species. *BMC Genomics*, 7(1), 171.

Levy Karin, E., Mirdita, M., & Söding, J. (2020). Metaeuk-sensitive, high-throughput gene discovery, and annotation for large-scale eukaryotic metagenomics. *Microbiome*, 8(1), 48.

Li, L., Dechesne, A., Madsen, J. S., Nesme, J., Sørensen, S. J., & Smets, B. F. (2020). Plasmids persist in a microbial community by providing fitness benefit to multiple phylotypes. *The ISME Journal*, 14(5), 1170–1181.

Li, W., & Godzik, A. (2006). Cd-hit: a fast program for clustering and comparing large sets of protein or nucleotide sequences. *Bioinformatics*, 22(13), 1658–1659.

Loftie-Eaton, W., Bashford, K., Quinn, H., Dong, K., Millstein, J., Hunter, S., Thomason, M. K., Merrikh, H., Ponciano, J. M., & Top, E. M. (2017). Compensatory mutations improve general permissiveness to antibiotic resistance plasmids. *Nature Ecology & Evolution*, 1(9), 1354–1363.

Long, A. M., Hou, S., Ignacio-Espinoza, J. C., & Fuhrman, J. A. (2021). Benchmarking microbial growth rate predictions from metagenomes. *The ISME Journal*, 15(11), 183–195.

Lynch, M., & Conery, J. S. (2003). The origins of genome complexity. *Science*, 302(5649), 1401–1404.

Margulies, M., Egholm, M., Altman, W. E., Attiya, S., Bader, J. S., Bemben, L. A., Berka, J., Braverman, M. S., Chen, Y.-J., Chen, Z., & et al. (2005). Genome sequencing in microfabricated high-density picolitre reactors. *Nature*, 437(7057), 376–380.

Menzel, P., Ng, K. L., & Krogh, A. (2016). Fast and sensitive taxonomic classification for metagenomics with kaiju. *Nature Communications*, 7, 11257.

Mihara, T., Nishimura, Y., Shimizu, Y., Nishiyama, H., Yoshikawa, G., Uehara, H., Hingamp, P., Goto, S., & Ogata, H. (2016). Linking virus genomes with host taxonomy. *Viruses*, 8(3), 66.

Millan, A. S., Peña-Miller, R., Toll-Riera, M., Halbert, Z. V., McLean, A. R., Cooper, B. S., & MacLean, R. C. (2014). Positive selection and compensatory adaptation interact to stabilize non-transmissible plasmids. *Nature Communications*, 5(1), 5208.

Moniruzzaman, M., Martinez-Gutierrez, C. A., Weinheimer, A. R., & Aylward, F. O. (2020). Dynamic genome evolution and complex virocell metabolism of globally-distributed giant viruses. *Nature Communications*, 11(11), 1–11.

Needham, D. M., Fichot, E. B., Wang, E., Berdjeeb, L., Cram, J. A., Fichot, C. G., & Fuhrman, J. A. (2018). Dynamics and interactions of highly resolved marine plankton via automated high-frequency sampling. *The ISME Journal*, (p. 1).

Needham, D. M., Poirier, C., Hehenberger, E., Jiménez, V., Swalwell, J. E., Santoro, A. E., & Worden, A. Z. (2019a). Targeted metagenomic recovery of four divergent viruses reveals shared and distinctive characteristics of giant viruses of marine eukaryotes. *Philosophical Transactions of the Royal Society B: Biological Sciences*, 374(1786), 20190086.

Needham, D. M., Yoshizawa, S., Hosaka, T., Poirier, C., Choi, C. J., Hehenberger, E., Irwin, N. A. T., Wilken, S., Yung, C.-M., Bachy, C., & et al. (2019b). A distinct lineage of giant viruses brings a rhodopsin photosystem to unicellular marine predators. *Proceedings of the National Academy of Sciences*, (p. 201907517).

Nurk, S., Meleshko, D., Korobeynikov, A., & Pevzner, P. A. (2017). metaspades: a new versatile metagenomic assembler. *Genome Research*, 27(5), 824–834.

Oliverio, A. M., Power, J. F., Washburne, A., Cary, S. C., Stott, M. B., & Fierer, N. (2018). The ecology and diversity of microbial eukaryotes in geothermal springs. *The ISME Journal*, 12(88), 1918–1928.

Olm, M. R., West, P. T., Brooks, B., Firek, B. A., Baker, R., Morowitz, M. J., & Banfield, J. F. (2019). Genome-resolved metagenomics of eukaryotic populations during early colonization of premature infants and in hospital rooms. *Microbiome*, 7(1), 26.

Olsen, G. J., Lane, D. J., Giovannoni, S. J., Pace, N. R., & Stahl, D. A. (1986). Microbial ecology and evolution: a ribosomal rna approach. *Annual Review of Microbiology*, 40, 337–365.

Ondov, B. D., Treangen, T. J., Melsted, P., Mallonee, A. B., Bergman, N. H., Koren, S., & Phillippy, A. M. (2016). Mash: fast genome and metagenome distance estimation using minhash. *Genome Biology*, 17(1), 132.

Pace, N. R., Stahl, D. A., Lane, D. J., & Olsen, G. J. (1986). The analysis of natural microbial populations by ribosomal rna sequences. In K. C. Marshall (Ed.) *Advances in Microbial Ecology*, Advances in Microbial Ecology, (p. 1–55). Springer US.

URL https://doi.org/10.1007/978-1-4757-0611-6_1

Parfrey, L. W., Walters, W. A., & Knight, R. (2011). Microbial eukaryotes in the human microbiome: ecology, evolution, and future directions. *Frontiers in Microbiology*, 2, 153.

Pawlowski, J., Audic, S., Adl, S., Bass, D., Belbahri, L., Berney, C., Bowser, S. S., Cepicka, I., Decelle, J., Dunthorn, M., & et al. (2012). Cbol protist working group: Barcoding eukaryotic richness beyond the animal, plant, and fungal kingdoms. *PLOS Biology*, 10(11), e1001419.

Pellow, D., Mizrahi, I., & Shamir, R. (2020). Plasclass improves plasmid sequence classification. *PLoS computational biology*, 16(4), e1007781.

Pronk, L. J., & Medema, M. H. (2022). Whokaryote: distinguishing eukaryotic and prokaryotic contigs in metagenomes based on gene structure. *Microbial Genomics*, 8(5), 000823.

Raoult, D., & Forterre, P. (2008). Redefining viruses: lessons from mimivirus. *Nature Reviews Microbiology*, 6(4), 315–319.

Ren, J., Ahlgren, N. A., Lu, Y. Y., Fuhrman, J. A., & Sun, F. (2017). Virfinder: a novel k-mer based tool for identifying viral sequences from assembled metagenomic data. *Microbiome*, 5, 69.

Ren, J., Song, K., Deng, C., Ahlgren, N. A., Fuhrman, J. A., Li, Y., Xie, X., Poplin, R., & Sun, F. (2020). Identifying viruses from metagenomic data using deep learning. *Quantitative Biology*. URL <https://doi.org/10.1007/s40484-019-0187-4>

Rodríguez-Beltrán, J., DelaFuente, J., León-Sampedro, R., MacLean, R. C., & San Millán, Á. (2021). Beyond horizontal gene transfer: the role of plasmids in bacterial evolution. *Nature Reviews Microbiology*, 19(6), 347–359.

Rondon, M. R., August, P. R., Bettermann, A. D., Brady, S. F., Grossman, T. H., Liles, M. R., Loiacono, K. A., Lynch, B. A., MacNeil, I. A., Minor, C., & et al. (2000). Cloning the soil metagenome: a strategy for accessing the genetic and functional diversity of uncultured microorganisms. *Applied and Environmental Microbiology*, 66(6), 2541–2547.

Roux, S., Enault, F., Hurwitz, B. L., & Sullivan, M. B. (2015). Virsorter: mining viral signal from microbial genomic data. *PeerJ*, 3, e985.

Royer, G., Decousser, J. W., Branger, C., Dubois, M., Médigue, C., Denamur, E., & Vallenet, D. (2018). Plascope: a targeted approach to assess the plasmidome from genome assemblies at the species level. *Microbial Genomics*, 4(9).

Schloissnig, S., Arumugam, M., Sunagawa, S., Mitreva, M., Tap, J., Zhu, A., Waller, A., Mende, D. R., Kultima, J. R., Martin, J., Kota, K., Sunyaev, S. R., Weinstock, G. M., & Bork, P. (2013). Genomic variation landscape of the human gut microbiome. *Nature*, 493(74307430), 45–50.

Schmidt, T. M., DeLong, E. F., & Pace, N. R. (1991). Analysis of a marine picoplankton community by 16s rrna gene cloning and sequencing. *Journal of Bacteriology*, 173(14), 4371–4378.

Schulz, F., Roux, S., Paez-Espino, D., Jungbluth, S., Walsh, D., Denef, V. J., McMahon, K. D., Konstantinidis, K. T., Eloe-Fadrosh, E. A., Kyrpides, N., & et al. (2020). Giant virus diversity and host interactions through global metagenomics. *Nature*, (p. 1–7).

Sedlar, K., Kupkova, K., & Provaznik, I. (2017). Bioinformatics strategies for taxonomy independent binning and visualization of sequences in shotgun metagenomics. *Computational and Structural Biotechnology Journal*, 15, 48–55.

Shi, Y., Zhang, H., Tian, Z., Yang, M., & Zhang, Y. (2018). Characteristics of arg-carrying plasmidome in the cultivable microbial community from wastewater treatment system under high oxytetracycline concentration. *Applied Microbiology and Biotechnology*, 102(4), 1847–1858.

Sieracki, M. E., Poulton, N. J., Jaillon, O., Wincker, P., Vargas, C. d., Rubinat-Ripoll, L., Stepanauskas, R., Logares, R., & Massana, R. (2019). Single cell genomics yields a wide diversity of small planktonic protists across major ocean ecosystems. *Scientific Reports*, 9(1), 1–11.

Slapeta, J., Moreira, D., & López-García, P. (2005). The extent of protist diversity: insights from molecular ecology of freshwater eukaryotes. *Proceedings. Biological Sciences*, 272(1576), 2073–2081.

Stein, J. L., Marsh, T. L., Wu, K. Y., Shizuya, H., & DeLong, E. F. (1996). Characterization of uncultivated prokaryotes: isolation and analysis of a 40-kilobase-pair genome fragment from a planktonic marine archaeon. *Journal of Bacteriology*, 178(3), 591–599.

Surville, C. A. (2005). Viruses in the sea. *Nature*, 437(7057), 356–361.

Surville, C. A. (2007). Marine viruses — major players in the global ecosystem. *Nature Reviews Microbiology*, 5(1010), 801–812.

Treangen, T. J., Sommer, D. D., Angly, F. E., Koren, S., & Pop, M. (2011). Next generation sequence assembly with amos. *Current Protocols in Bioinformatics, Chapter 11*, Unit 11.8.

Venter, J. C., Remington, K., Heidelberg, J. F., Halpern, A. L., Rusch, D., Eisen, J. A., Wu, D., Paulsen, I., Nelson, K. E., Nelson, W., & et al. (2004). Environmental genome shotgun sequencing of the sargasso sea. *Science (New York, N.Y.)*, 304(5667), 66–74.

Vergin, K. L., Urbach, E., Stein, J. L., DeLong, E. F., Lanoil, B. D., & Giovannoni, S. J. (1998). Screening of a fosmid library of marine environmental genomic dna fragments reveals four clones related to members of the order planctomycetales. *Applied and Environmental Microbiology*, 64(8), 3075–3078.

Vorobev, A., Dupouy, M., Carradec, Q., Delmont, T. O., Annamalé, A., Wincker, P., & Pelletier, E. (2020). Transcriptome reconstruction and functional analysis of eukaryotic marine plankton communities via high-throughput metagenomics and metatranscriptomics. *Genome Research*, 30(4), 647–659.

West, P. T., Probst, A. J., Grigoriev, I. V., Thomas, B. C., & Banfield, J. F. (2018). Genome-reconstruction for eukaryotes from complex natural microbial communities. *Genome Research*, 28(4), 569–580.

Wilhelm, S. W., & Surville, C. A. (1999). Viruses and nutrient cycles in the seaviruses play critical roles in the structure and function of aquatic food webs. *BioScience*, 49(10), 781–788.

Woese, C. R., & Fox, G. E. (1977). Phylogenetic structure of the prokaryotic domain: the primary kingdoms. *Proceedings of the National Academy of Sciences of the United States of America*, 74(11), 5088–5090.

Wolska, K. I. (2003). Horizontal dna transfer between bacteria in the environment. *Acta Microbiologica Polonica*, 52(3), 233–243.

Xia, L. C., Steele, J. A., Cram, J. A., Cardon, Z. G., Simmons, S. L., Vallino, J. J., Fuhrman, J. A., & Sun, F. (2011). Extended local similarity analysis (elsa) of microbial community and other time series data with replicates. *BMC Systems Biology*, 5(2), S15.

Zheng, J., Guan, Z., Cao, S., Peng, D., Ruan, L., Jiang, D., & Sun, M. (2015). Plasmids are vectors for redundant chromosomal genes in the *bacillus cereus* group. *BMC Genomics*, 16(1), 6.

Zhou, F., & Xu, Y. (2010). cbar: a computer program to distinguish plasmid-derived from chromosome-derived sequence fragments in metagenomics data. *Bioinformatics*, 26(16), 2051–2052.